Title:
Modeling Oceanic Primary Production: Photoacclimation and Nutrient Effects on Light-saturated Photosynthesis

Journal:
Marine Ecology Progress Series

PI:
Michael Behrenfeld

Popular Summary:
In this report, we describe a new model (the "PhotoAcc" model) for estimating changes in the light-saturated rate of chlorophyll-normalized phytoplankton carbon fixation (Pbmax). The model is based on measurements conducted during the Atlantic Meridional Transect studies and the Bermuda Time Series program. The PhotoAcc model explained 64% to 82% of the observed variability in Pbmax for our data set, whereas none of the previously published Pbmax models described over the past 44 years explained any of the variance. The significance of this result is that a primary limiting factor for extracting ocean carbon fixation rates from satellite measurements of near surface chlorophyll has been errors in the estimate of Pbmax. Our new model should thus result in much improved calculations of oceanic photosynthesis and thus the role of the oceans in the global carbon cycle.

Significant Findings:
Description of primary sources of variability in the critical model parameter Pbmax.

Running Head: Modeling Phytoplankton Photosynthesis

Modeling Oceanic Primary Production: Photoacclimation and nutrient effects on light-saturated photosynthesis

Michael J. Behrenfeld[1], *Emilio Marañón*[2], *David A. Siegel*[3], *Stanford B. Hooker*[1]

1 National Aeronautics and Space Administration, Goddard Space Flight Center, Code 971, Building 33, Greenbelt, MD. 20771, USA

2 Departamento de Ecología y Biología Animal, Universidad de Vigo, E-36200 Vigo, Spain

3 Institute for Computational Earth System Science, University of California, Santa Barbara, Santa Barbara, CA 93106-3060, USA

Key Words: Photosynthesis, Modeling, Phytoplankton

October 17, 2000

ABSTRACT

Availability of remotely-sensed phytoplankton biomass fields has greatly advanced primary production modeling efforts. However, conversion of near surface chlorophyll concentrations to carbon fixation rates has been hindered by uncertainties in modeling light-saturated photosynthesis (P^b_{max}). Here, we introduce a physiologically-based model for P^b_{max} that focuses on the effects of photoacclimation and nutrient limitation on relative changes in cellular chlorophyll and CO_2 fixation capacities. This 'PhotoAcc' model describes P^b_{max} as a function of light level at the bottom of the mixed layer or at the depth of interest below the mixed layer. Nutrient status is assessed from the relationship between mixed layer and nutricline depths. Temperature is assumed to have no direct influence on P^b_{max} above 5°C. The PhotoAcc model was parameterized using photosynthesis-irradiance observations made from extended transects across the Atlantic ocean. Model performance was validated independently using time-series observations from the Sargasso Sea. The PhotoAcc model explained 64% to 82% of the variance in light-saturated photosynthesis. Previously described temperature-dependent models did not account for a significant fraction of the variance in P^b_{max} for our test data sets.

INTRODUCTION

Photosynthesis is a fundamental process of nearly all known ecosystems, such that the level of photoautotrophic carbon fixation supported by a given environment broadly dictates the local biomass of subsequent trophic levels and the biogeochemical exchange of elements between systems. Models of biospheric primary production have been greatly aided by global-scale satellite observations (Field et al. 1998), but conversion of measured plant biomass to net

photosynthesis has remained problematic. Whereas terrestrial productivity models suffer from a lack of observational data for parameterization and testing (Field et al. 1998), high-sensitivity measurements of net primary production in aquatic systems have been routine since the introduction of the ^{14}C method by Steemann-Nielsen (1952).

Analyses of vertical profiles of phytoplankton photosynthesis revealed early on that, when normalized to depth-specific chlorophyll concentrations, primary production can be modeled to first order simply as a function of subsurface irradiance (Ryther 1956; Ryther and Yentsch 1957; Talling 1957). A variety of analytical expressions were subsequently developed describing this relationship between vertical light attenuation and chlorophyll-normalized carbon fixation (reviewed by: Platt and Sathyendranath 1993; Behrenfeld and Falkowski 1997a). Such models account for most of the observed variance in depth-integrated photosynthesis (ΣPP) (particularly when measurements encompass a wide phytoplankton biomass range) provided model input includes three critical features of the water column: (1) the vertical distribution of chlorophyll, (2) the downwelling attenuation coefficient (K_d) for photosynthetically active radiation (PAR), and (3) the maximum carbon fixation rate per unit of chlorophyll (P^b_{opt}) (Behrenfeld and Falkowski 1997a,b).

For over 40 years, developments in phytoplankton primary production models have focused on refining characterizations of the above three critical water column features, with clearly the greatest achievements realized in the description of the underwater light field (e.g., Morel 1991; Platt and Sathyendranath 1988; Antoine et al. 1996). Progress has also been made in predicting vertical profiles of chlorophyll (Morel and Berthon 1989; Platt and Sathyendranath 1988), but models of P^b_{opt} have remained rudimentary and entirely inconsistent (Behrenfeld and

Falkowski 1997a). The importance of accurate P^b_{opt} estimates can not be overstated, especially when model performance is evaluated by comparison with point-source field observations. For globally representative data sets, phytoplankton biomass alone accounts for < 40% of ΣPP variability, while inclusion of measured P^b_{opt} values can increase explained variance in ΣPP to > 80% (Balch and Byrne 1994; Behrenfeld and Falkowski 1997b). In oligotrophic regions where the range in chlorophyll concentration is further constrained, accurate estimates of P^b_{opt} are even more critical (Banse and Yong 1990; Siegel et al. 2000).

The function of P^b_{opt} models is to capture spatial and temporal changes in assimilation efficiencies (i.e., carbon fixed per unit of chlorophyll) resulting from physiological acclimation to environmental variability. Currently, the two principle approaches for estimating P^b_{opt} in regional- to global-scale models are: (1) to assign fixed, climatological values to biogeographical provinces (Longhurst et al. 1995; Longhurst 1995) and (2) to define predictive relationships between P^b_{opt} and one or more environmental variable(s) (e.g., temperature, nutrient concentration) (Megard 1972; Balch et al. 1992; Antoine et al. 1996; Behrenfeld and Falkowski 1997b). Both techniques have advantages, but differ in their intended application. For example, the first approach furnishes broad-scale average values for designated regions and is not intended to accurately reproduce the much finer scale physiological variability in ^{14}C-uptake rates corresponding to a given day, depth, and location. As for the second approach, an effective model should, ideally, provide P^b_{opt} estimates comparable at this point-source scale of field measurements, but a successful model of this genre has not yet been described.

Here we introduce a model, belonging to this second category, that captures P^b_{opt} variability in natural phytoplankton assemblages. The model largely focuses on changes in P^b_{opt}

resulting from photoacclimation and is thus referred to as the 'PhotoAcc Model', although a nutrient-dependence is also prescribed. In the following section, the conceptual basis and underlying equations of the PhotoAcc model are presented. We then describe field data used for model parameterization and testing, along with our approach to assessing nutrient status and photoacclimation irradiance. The PhotoAcc model assumes P^b_{opt} to be temperature-independent. Our rationale for this divergence from previous treatments is given in the Synthesis section, along with an assessment of model limitations, directions for expansion, and potential avenues for global implementation.

THE PHOTOACC MODEL

Phytoplankton carbon fixation is commonly measured under ambient light conditions during ≈6 to 24 h *in situ* or simulated *in situ* incubations. With this technique, the water column is treated as a compound photosynthetic unit, yielding depth-dependent relationships between photosynthesis and subsurface irradiance. The variable, P^b_{opt}, is defined as the maximum rate of chlorophyll-normalized carbon fixation measured in the water column using this technique (Wright 1959; Behrenfeld and Falkowski 1997b). A single P^b_{opt} value is thus obtained for each vertical profile (note: the superscript 'b' denotes normalization to chlorophyll). Photosynthesis-irradiance (PI) measurements can also be conducted on field samples and involve ≈0.5 to 2 h incubations under a range of constant light intensities. This method yields unique P^b_{max} values for each population sampled within the water column. The variable, P^b_{max}, is defined as the light-saturated photosynthetic rate and is constrained by the capacity of the Calvin cycle reactions, which fix CO_2 into carbohydrates (Stitt 1986; Sukenik et al. 1987; Orellana and Perry

1992).

Distinction between P^b_{max} and P^b_{opt} was recommended by Behrenfeld and Falkowski (1997b) because P^b_{max} is measured under fixed light conditions that maintain a constant photosynthetic rate throughout an incubation, whereas P^b_{opt} is measured under natural fluctuating light which causes photosynthesis to vary from light-limited to light-saturated to photoinhibited during an incubation. Nevertheless, P^b_{opt} is generally observed near the surface where photosynthesis is maintained at P^b_{max} for most of the photoperiod. Thus, unless photoinhibition is excessive or ambient PAR is very low, an effective model for P^b_{max} will likewise provide robust estimates of P^b_{opt}. We designed the PhotoAcc model to specifically describe the changes in chlorophyll and Calvin cycle capacity (P_{max}) that result in P^b_{max} variability, but we apply the model equally for estimating both P^b_{max} and P^b_{opt}.

Modeling P^b_{max}

A central tenet of the PhotoAcc model is that phytoplankton adjust the capacity of the Calvin cycle (P_{max}) to provide sufficient reduced carbon products within a given photoperiod to meet the diel demands for cell maintenance and growth. Chlorophyll concentration is considered, to first order, a dependent function of P_{max}, since the primary role of light harvesting is to support the ATP and NADPH demands of the Calvin cycle. Consequently, the ratio of P_{max} to chlorophyll (i.e., P^b_{max}) is somewhat insensitive to changes in growth conditions, except when these changes shift the balance between light harvesting and carbon fixation. Effectively modeling P^b_{max} is therefore simply a matter of describing changes in chlorophyll *relative* to the Calvin cycle capacity. In this sense, modeling P^b_{max} is less complicated than estimating

photosynthesis per cell or unit of carbon, since it does not require knowledge of growth-rate- or species-dependent variability in cell volume or carbon:chlorophyll ratios.

The PhotoAcc model focuses on two primary sources of variability in P^b_{max}: light and nutrient availability. Light is assumed to influence P^b_{max} because changes in irradiance cause light harvesting to vary independently of the Calvin cycle capacity. The relationship between chlorophyll and growth irradiance was derived from laboratory-based measurements on 23 phytoplankton species described in 23 studies from the literature. Reported irradiances were converted to units of μmol quanta m^{-2} s^{-1} following Richardson et al. (1983). Data from a given study were binned according to species, photoperiod, and growth temperature and then each bin divided by a scalar to yield normalized chlorophyll concentrations (Chl_{norm}). For our 342 observations, Chl_{norm} exhibited a dependence on growth irradiance (I_g) following (Fig. 1):

$$Chl_{norm} = a + b \times e^{-c \times Ig}. \qquad \text{(Eq. 1)}$$

Equation 1 was used to describe changes in P^b_{max} resulting from irradiance-dependent change in chlorophyll. However, values for the parameters (a,b,c) were derived from field measurements of P^b_{max}, rather than our laboratory-based data set (Fig. 1), because the PhotoAcc model aims to describe changes in chlorophyll relative to the Calvin cycle, not chlorophyll per cell. The critical features of equation 1 are the prediction of an intercept when I_g approaches zero and the asymptotic decrease to a minimum value at very high light (Fig. 1).

Nutrient-dependence of P^b_{max} is assumed to result from an increase in the energetic cost of extracting nutrients from the surrounding medium as concentrations decrease. An associated increase in light harvesting for ATP generation, rather than carbon fixation, will thus shift the balance between chlorophyll and P_{max}, causing P^b_{max} to decrease. Few laboratory studies have

specifically addressed this issue of nutrient-dependent changes in the relative abundance of photosynthetic components. Falkowski et al. (1989) reported Calvin cycle and light harvesting components to initially decrease in parallel with nitrogen-limited growth and then to shift to a new equilibrium when growth rate was reduced by > 40%. This initial insensitivity to nutrient limitation supports our hypothesis that normalization of P_{max} to chlorophyll conveys a level of resilience in P^b_{max} to environmental variability, while the eventual shift indicates a sensitivity of P^b_{max} to nutrients at vanishingly low concentrations.

Model Summary

All of the relationships involved in the PhotoAcc model are illustrated in figure 2. For phytoplankton in a surface mixed layer where growth is not strongly nutrient limited, P_{max} is assigned an irradiance-independent value of 1 mgC m^{-3} h^{-1}. Changes in chlorophyll are expressed relative to this P_{max} value using equation 1, where I_g is taken as the average daily PAR at the bottom of the mixed layer. Thus, P^b_{max} is modeled simply as an inverse function of chlorophyll under these conditions (Fig. 2a). Below the mixed layer, changes in chlorophyll are described using the same formulation as within the mixed layer, except that I_g is taken as the average daily PAR at the depth of interest. P_{max} below the mixed layer is again assigned a value of 1 mgC m^{-3} h^{-1} at high light, but then assumed to decrease at very low light (Fig. 2a - inset). This relationship between P_{max} and I_g was described by:

$$P_{max} = d + f \times (1 - h^{n \times Ig}), \qquad \text{(Eq. 2)}$$

where d, f, h, and n are parameters and n has inverse units of I_g to yield a dimensionless exponent. A low-light decrease in P_{max} below the mixed layer is prescribed because a high

Calvin cycle capacity is unnecessary in chronically light-limited phytoplankton deep within a stratified water column (Geider et al. 1986; Orellana and Perry 1992). A similar light-dependent decrease in P_{max} is not assumed for phytoplankton in a deep mixing layer because maintaining a high Calvin cycle capacity enables enhanced carbon fixation during periodic exposures to high light near the surface.

Relative to nutrient sufficient conditions, chlorophyll is assumed to increase more slowly with decreasing irradiance in nutrient stressed phytoplankton. The consequential reduction in light harvesting at low light thus reduces Calvin cycle requirements and causes P_{max} to vary as a function of irradiance (Fig. 2b). The chlorophyll-irradiance relationship for nutrient stressed conditions was again modeled using the same parameters as nutrient sufficient conditions except that a lower slope (b') was assigned. Irradiance-dependent changes in P_{max} were described using equation 2. Finally, the enhanced costs of acquiring nutrients described above was effectuated by assigning a lower value to P_{max} across all light levels compared to nutrient sufficient conditions (Fig. 2).

Chlorophyll and P_{max} relationships for the three conditions of the PhotoAcc model (Fig. 2) are all expressed relative to the constant P_{max} value of 1 mgC m^{-3} h^{-1} for nutrient sufficient, mixed layer phytoplankton. Parameterizing these equations with field measurements of P^b_{max} required an environmental index of nutrient status and an assessment of surface mixing depths. Our approach to these issues and the field data employed are detailed in the following section.

METHODS

Field data

The consummate objective in developing a P^b_{max} model is to achieve effective estimates that are robust to variations in environmental conditions and taxonomic composition. To this end, field measurements conducted during the Atlantic Meridional Transect (AMT) program provided a suite of complimentary physical, chemical, and biological observations from a diversity of oceanographic regimes. We employed results from two of these program transects, AMT-2 (22 April - 22 May, 1996) and AMT-3 (16 Sept. - 25 Oct., 1996); each spanning an 11,000 km region between the United Kingdom and Falkland Islands. In addition to encompassing 5 of the major biogeochemical provinces defined by Longhurst et al. (1995), the AMT studies were also ideal for model parameterization because they exhibited significantly divergent latitudinal patterns in P^b_{max} despite being nearly identical geographical transects (Marañón and Holligan 1999; Marañón et al. 2000).

Protocols employed for optical and biological measurements during AMT-2 and AMT-3 have been previously reported (Robins et al. 1996; Marañón and Holligan 1999; Marañón et al. 2000). Optical measurements were conducted using the SeaWiFs Optical Profiling System (SeaOPS) with a set of 7-channel light sensors (Robins et al. 1996). Optical measurements with the SeaOPS have a characteristic uncertainty of 3.4%, with 1.5% of this from ship-shadow contamination (Hooker and Maritorena 2000). Photosynthesis-irradiance measurements were conducted on samples collected at each station from 7 m, near the base of the mixed layer, and near the chlorophyll maximum (Marañón and Holligan 1999). This sampling strategy provided P^b_{max} values from within and below the mixed layer. Data collected between 40°N and 49°N during AMT-2 were not used in our analysis due to inconsistencies between results from different chlorophyll measurement techniques, nor did we use the 60 m sample from 38°S during

AMT-3, due to considerable divergence between chlorophyll concentration and spectral attenuation coefficients ($K_{d\lambda}$).

PhotoAcc model performance was additionally tested using a 6-year record of light and primary production from the U.S.-JGOFS Bermuda Atlantic Time Series (BATS) program and Bermuda BioOptics Program (BBOP). BATS and BBOP measurement protocols have been described previously (Knap et al. 1993; Michaels and Knap 1996; Siegel et al. 1995a,b, 2000). Chlorophyll normalized rates of primary production (P^b) were based on light-dark *in situ* ^{14}C-uptake measurements conducted from sunrise to sunset and HPLC determinations of phytoplankton pigment. Each vertical profile of P^b was visually inspected to extract the appropriate value for P^b_{opt}. With few exceptions, P^b_{opt} was taken as the P^b value measured at 20 m. Above this depth, a slight photoinhibitory effect was common, while P^b values below 20 m generally decreased due to longer periods of light-limited photosynthesis. On a few occasions, the P^b value at 20 m greatly exceeded the measured values immediately above and below this depth, in which case the second highest P^b value was taken as P^b_{opt}.

Nutrient Limitation Index

The PhotoAcc model requires an environmental index to indicate when P^b_{max} should be modeled as nutrient 'charged' (Fig. 2a) or 'depleted' (Fig.2b). Over a majority of the open ocean, the dissolved concentration of nutrients is not an effective index of nutrient stress because the daily allocation of resources available for growth is largely determined by food web recycling rates. We therefore employed the relationship between the physical mixed layer depth (Z_M) and the nutricline depth (Z_N) as an alternative, first-order index of nutrient status. The basis

for this index is that, when a physical forcing (e.g., a storm) deepens the mixed layer such that mixing penetrates the nutricline, the upper water column becomes 'charged' with nutrients and either a close correspondence exists between Z_M and Z_N or nutrients are elevated throughout the water column. When stratification follows, the mixed layer shoals and Z_M separates from Z_N. Recycling inefficiencies in this stratified system will result in a coincident export of nutrients out of the active biological pool and into particulate refractory and deep-ocean pools. Correspondence in time scales for these two events will thus allow separation of Z_N and Z_M to function as a correlate for increasing nutrient stress.

Clearly, conditions will exist when $Z_N > Z_M$, yet recycling is sufficient to transiently maintain phytoplankton in a nutrient 'charged' physiological state. The relationship between Z_N and Z_M was thus treated as a first-order index to separate nutrient 'charged' from 'depleted' data. For this analysis, Z_M was evaluated from vertical profiles of density (σ_t) and Z_N assigned the depth at which NO_3^- was first detected. For nearly the entire AMT-3 transect, either a close correspondence existed between Z_M and Z_N or NO_3^- was detectable to the surface (Fig. 3a). The AMT-3 data were thus used to parameterize the nutrient 'charged' PhotoAcc equations (Fig. 2a). During AMT-2, a general separation of Z_M and Z_N occurred between 30°N and 42°S (Fig. 3b) and provided the data for parameterizing the nutrient 'depleted' relationships (Fig. 2b).

Photoacclimation Depths

The PhotoAcc model requires an assessment of the mixing depth to which surface phytoplankton are photoacclimated (Z_{ACCL}). We determined Z_{ACCL} by visually inspecting vertical profiles of σ_t, NO_3^-, PO_4^{3-}, and chlorophyll for each sampling date and location and assigning

Z_{ACCL} the shallowest depth at which a vertical gradient was observed in any of these four water column properties. Invariably, Z_{ACCL} corresponded to the depth of Z_M under nutrient 'depleted' conditions (Fig. 4a). Typically, σ_t, NO_3^-, PO_4^{3-}, and chlorophyll all indicated a similar depth for Z_{ACCL} under nutrient 'charged' conditions (Fig. 4b). However, occasionally when Z_M was large, nutrient and chlorophyll profiles indicated a shallower depth for Z_{ACCL} than σ_t (Fig. 4c). This infrequent condition likely corresponds to a period shortly after a deep mixing event when physical forcing on the system has relinquished and the upper water column is beginning to stratify.

RESULTS

The Parameterized PhotoAcc Model

Similarity between chlorophyll-irradiance relationships for the 3 conditions of the PhotoAcc model (Fig. 2) allowed parameterization through a stepwise procedure. For each step, I_g (mol quanta m^{-2} h^{-1}) was calculated for the depth of Z_{ACCL} (m) using measured surface PAR (mol quanta m^{-2} h^{-1}) and spectral downwelling attenuation coefficients ($K_{d\lambda}$: m^{-1}). Chlorophyll and P_{max} relationships were fit to AMT data using equations 1 and 2. Parameter values with the smallest number of significant digits were chosen that yielded fits to the observational data that were not significantly different than least-squares derived parameters.

Step 1: Mixed Layer, Nutrient 'Charged': For this condition, P_{max} is constant (1 mgC m^{-3} h^{-1}) and P^b_{max} (mgC (mg Chl)$^{-1}$ h^{-1}) varies solely as a function of chlorophyll (Fig. 2a). The relationship between chlorophyll and I_g was thus derived from measured P^b_{max}, since Chl_{norm} =

$P_{max} \times {P^b}_{max}^{-1} = {}^1/{P^b}_{max}$. Fitting equation 1 to the inverse of ${P^b}_{max}$ as a function of I_g yielded:

$$Chl_{norm} = 0.036 + 0.3 \times e^{-3 \times Ig}, \quad \text{(Eq. 3)}$$

where parameter units from equation 1 are: a = mgChl m^{-3}, b = mgChl m^{-3}, and c = $m^2 \times h \times$ (mol quanta)$^{-1}$.

Step 2: Sub-mixed Layer, Nutrient 'Charged': Equation 3 provides the chlorophyll-irradiance relationship for calculating ${P^b}_{max}$ below the mixed layer. Thus, the decrease in P_{max} at vanishingly low light (Fig. 2a-inset) was derived from the difference between measured ${P^b}_{max}$ and the inverse of equation 3. Fitting equation 2 to this difference as a function of I_g yielded:

$$P_{max} = 0.1 + 0.9 \times [1 - (5 \times 10^{-9})^{Ig}], \quad \text{(Eq. 4)}$$

where parameter units from equation 2 are: d,f = mgC m^{-3} h^{-1}, h = unitless, and n = 1 $m^2 \times h$ (mol quanta)$^{-1}$. I_g in equation 4 is the average daily PAR at the depth of interest below the mixed layer.

Step 3: Nutrient 'Depleted' Water Column: The chlorophyll and P_{max} relationships in this model (Fig. 2b) are used for estimating ${P^b}_{max}$ from the surface to Z_N in nutrient 'depleted' regions. The model employs a chlorophyll-irradiance relationship with the same parameter values as equation 3 except for a lower slope (b'). The nutrient 'depleted' model was thus parameterized by fitting b' and equation 2 to the inverse of ${P^b}_{max}$ as a function of I_g for the AMT-2 data collected between 30°N and 42°S (Fig. 3b). The resultant relationships were:

$$Chl_{norm} = 0.036 + 0.15 \times e^{-3 \times Ig} \quad \text{(Eq. 5)}$$

and

$$P_{max} = 0.15 + 0.3 \times (1 - 0.25^{lg}). \quad \text{(Eq. 6)}$$

In this case, parameters chosen for describing the irradiance-dependence of Chl_{norm} and P_{max} do not represent unique mathematical solutions, as equations 1 and 2 were fit simultaneously to the observational data.

Model Performance

Equations 3 through 6 encompass the complete set of relationships necessary for estimating P^b_{max} with the PhotoAcc model. Comparison of modeled versus measured P^b_{max} values for nutrient 'charged' regions of the AMT transects indicated that an effective representation of spatial variability was achieved both above (Fig. 3c,d) and below (Fig. 3e,f) Z_{ACCL} (solid black symbols in Fig. 3). Likewise, the nutrient 'depleted' model yielded spatial patterns in P^b_{max} consistent with those measured above (Fig. 3d) and below (Fig. 3f) Z_{ACCL} for the AMT-2 region between 30°N and 42°S (gray symbols in Fig. 3). Overall, the PhotoAcc model captured 75% of the observed variance in P^b_{max} for AMT-2 and AMT-3.

Effectiveness of the PhotoAcc model at estimating P^b_{opt} was evaluated using the 6 year BATS/BBOP data set (Fig. 5). For these data, a single P^b_{opt} value was extracted from each monthly profile of P_z. The near-surface location of P^b_{opt} (≈20 m) and minimal photoinhibition ensured that light-saturated photosynthesis (P^b_{max}) was maintained during each measurement over most of the photoperiod. P^b_{max} was calculated for each month using both the nutrient 'charged' and 'depleted' models. The nutrient 'charged' model provided the best estimates of P^b_{opt} during and shortly following the seasonal deep mixing events evidenced in profiles of Z_M and Z_N (solid black symbols in Fig. 5a). These winter mixing events were followed each year by

a period of increasing stratification, where Z_M gradually separated from Z_N (Fig. 5b). Accordingly, the nutrient 'depleted' model generally provided the best estimates of P^b_{opt} during these stratified periods (gray symbols in Fig. 5a). Overall, the PhotoAcc model captured 82% of the variance in P^b_{opt} for the BATS data set.

Comparison with Temperature-dependent P^b_{opt} Models

Most regional- and global-scale models for P^b_{opt} are simple functions of sea surface temperature (excepting: Balch and Byrne 1994; Longhurst 1995), with considerable variability between models (Behrenfeld and Falkowski 1997a). The AMT and BATS studies encompassed a wide range of sea surface temperatures (5°C to 28°C) and thus provided an opportunity to compare the PhotoAcc model with the temperature-dependent models of Megard (1972), Balch et al..(1992), Behrenfeld and Falkowski (1997b), and Antoine et al. (1996) (Fig. 6). Such a comparison requires an objective basis for applying the nutrient 'charged' or 'depleted' PhotoAcc equations. As shown in figures 3 and 5, the nutrient 'charged' model occasionally provided a better estimate of measured P^b_{max} and P^b_{opt} when Z_M was separated from Z_N, and visa versa. If switching between models is instead strictly based on the correspondence of Z_M and Z_N, the PhotoAcc model captures 64% of the variance in P^b_{max} and P^b_{opt} for AMT and BATS (Fig. 6e). This value is slightly lower than the best fit PhotoAcc results (Fig. 6f), but still a vast improvement over the temperature-dependent models which yielded a maximum correlation coefficient of $r^2 = 0.07$ (Fig. 6a-d). Results of this comparison thus indicate that (1) the PhotoAcc model addresses significant sources of variability in P^b_{max} and P^b_{opt} not captured by the temperature-dependent functions and (2) performance of the PhotoAcc will improve if our first-

order index of nutrient stress can be replaced with a more quantitative index.

SYNTHESIS

The importance of effectively modeling light-saturated photosynthesis at the difficult local scale of daily primary production measurements has been recognized for over 40 years (Ryther 1956; Ryther and Yentsch 1957). The most common approach to this problem has been to describe P^b_{opt} as a function of temperature. Such models capture a fraction of the observed variability in P^b_{opt} because temperature is weakly correlated with causative environmental forcing factors. In contrast, the PhotoAcc model attempts to explicitly describe primary causative relationships at the level of chlorophyll synthesis and changes in the Calvin cycle capacity. With this approach, the model effectively reproduced spatial and temporal variability in light-saturated photosynthesis for the AMT and BATS studies. These field programs do not, however, fully encompass global nutrient, light, and temperature conditions. In the following sections, we evaluate the predictions and hypotheses of the PhotoAcc model, discuss potential alterations to account for additional growth constraints, and propose avenues for global implementation.

Maximum Light-saturated Photosynthesis

The PhotoAcc model predicts a maximum photosynthetic rate of $P^b_{max} = 1/0.036 = 27.5$ mgChl m^{-3} (Eq. 3), corresponding to nutrient 'charged', high light conditions. Falkowski (1981) proposed a maximum value of 25 mgC $mgChl^{-1}$ h^{-1} by assuming a minimum photosynthetic unit (PSU_{O2}) size of 2000 chlorophyll molecules per O_2 evolved and a PSU_{O2} turnover time (τ) of 1

ms. Choosing a lower PSU_{O2} or τ value would yield a higher maximum for P^b_{max}. Laboratory measurements suggest that PSU_{O2} can range from 300 to 5000 chl O_2^{-1} (Falkowski et al. 1981), while τ may vary from $\geq$ 5 ms to slightly less than 2 ms (Falkowski et al. 1981; Behrenfeld et al. 1998) depending on the excess capacity of the photosystems (Kok 1956; Weinbaum et al. 1979; Heber et al. 1988; Leverenz et al. 1990; Behrenfeld et al. 1998). Thus, a potential exists for P^b_{max} to exceed 25 mgC mgChl^{-1} h^{-1}, although values > 20 mgC mgChl^{-1} h^{-1} are rarely observed in the laboratory [e.g., Glover (1980) reported values between 1.6 and 21 mgC mgChl^{-1} h^{-1} for 11 species]. In the field, P^b_{max} (or P^b_{opt}) values in excess of 20 mgC mgChl^{-1} h^{-1} are occasionally reported that exhibit well defined diurnal patterns (e.g., Malone et al. 1980; Hood et al. 1991). In conclusion, the PhotoAcc maximum for P^b_{max} of 27.5 mgC mgChl^{-1} h^{-1} is close to the theoretical value proposed by Falkowski (1981), is well within the range of variability suggested by laboratory measurements of PSU_{O2} and τ, and is consistent with maximum values reported from previous field studies.

Temperature Revisited

We consider temperature to have a negligible direct influence on P^b_{max} above 5°C for the following reasons: (1) Laboratory studies with phytoplankton monocultures indicate clear temperature dependence for maximum algal growth rates (Eppley 1972), but a variable, species-dependent influence on P^b_{max} (e.g., Steemann-Nielsen and Hansen 1959; Steemann-Nielsen and Jørgensen 1968; Harris 1978; Morris 1981; Post et al. 1985). Enzymatic temperature optima differ between species according to the ambient temperature from which they were isolated. Thus, in field samples with taxonomically diverse phytoplankton assemblages acclimated to

their ambient conditions, temperature dependence of P^b_{max} is likely tempered. (2) Although the activity of Calvin cycle enzymes, such as ribulose-1-5-bisphosphate carboxylase (Rubisco), exhibit classic Arrhenius temperature dependence, decreases in activity at lower temperatures may be offset by increasing enzyme concentrations (Steemann-Nielsen and Hansen 1959; Steemann-Nielsen and Jørgensen 1968; Geider et al. 1985; Geider 1987). In other words, sensitivity of P^b_{max} to temperature may be diminished if increases in enzyme concentration keep pace with decreasing activities at lower temperatures. (3) Temperature-dependent changes in the Calvin cycle capacity may be paralleled by changes in chlorophyll (e.g., Durbin 1974; Yoder 1979; Verity 1981; Lapointe et al. 1984), such that normalization of P_{max} to chlorophyll masks temperature dependence.

Below 5°C, the physiological adjustments described above may not be sufficient to eliminate temperature effects on P^b_{max}. Currently, the minimum mixed layer P^b_{max} value predicted by the PhotoAcc model is 3 mgC $mgChl^{-1}$ h^{-1}. This value is near the maximum P^b_{opt} value (< 0.5 to ≈3 mgC $mgChl^{-1}$ h^{-1}) reported by Dierssen et al. (2000) for Antarctic phytoplankton sampled from -2°C to 2°C waters. Low P^b_{opt} values measured in the Southern ocean partly result from prolonged periods of subsaturated photosynthesis causing a weaker relationship between P^b_{max} and P^b_{opt}. Nevertheless, a direct temperature effect is also likely and could be accounted for in the PhotoAcc model by expressing nutrient 'charged' P_{max} as a temperature-dependent variable. For example, the following relation (where T = temperature):

$$P_{max} = 0.4 + 0.6 \times [1 - \exp^{-0.6 \times (T + 6)}]^{50} \quad \text{(Eq. 8)}$$

would provide a temperature-dependent decrease in P^b_{max} below 5°C while essentially leaving modeled values unaltered above 5°C.

Acclimation Irradiance (I_g)

Modeling photoacclimation as a function of light at the bottom of the mixed layer is mathematically the simplest formulation, but its physiological representation is dependent on the kinetic balance between responses to low- and high-light. Specifically, if photoacclimation follows first-order kinetics with similar rate constants for both high- and low-light, P^b_{max} will vary as a function of the average light in the mixed layer (Falkowski and Wirick 1981; Lewis et al. 1984; Cullen and Lewis 1988). Likewise, P^b_{max} will scale to an irradiance less than the average if responses to low-light are stronger (Cullen and Lewis 1988) and to higher than average light if high-light effects dominate (Vincent et al. 1994; Geider et al. 1996).

Photoacclimation rate constants are typically derived from laboratory 'light-shift' experiments, where cells acclimated for multiple generations to a given irradiance are transferred to much higher or lower light (e.g., Lewis et al. 1984). Riper et al. (1979) suggested that decreases in cellular chlorophyll following a shift to high-light result from (1) dilution by coincident cell division and cessation of chlorophyll synthesis, (2) photooxidation, and (3) enzymatic breakdown. If these three processes combine to yield a kinetic response of similar magnitude and opposite sign as a shift to low light (Lewis et al. 1984), then phytoplankton must acclimate to the average light in the mixed layer by continuously synthesizing and degrading chlorophyll at time scales of < 1 h as they transit between the surface and Z_{ACCL}. However, light-shift experiments do not mimic natural conditions well, since mixed layer phytoplankton are preconditioned to periodic high light exposures and thus are physiologically poised to effectively dissipate excess excitation energy (Behrenfeld et al. 1998). Goericke and Welschmeyer (1992) demonstrated that chlorophyll turnover is independent of light level in

preconditioned cells and conclude that photooxidation and enzymatic degradation of chlorophyll are artifacts of light-shift experiments. Chlorophyll synthesis at subsaturating light (Escoubas et al. 1995) should thus dominate over the dilution effect of cell division and cause photoacclimation to scale to a lower than average light level. This conclusion implies that cellular chlorophyll is not synthesized and degraded at an hourly time scale, but rather changes at the longer time scale of mixed layer deepening and shoaling. Clearly, additional analyses with mixed layer phytoplankton are needed to further resolve photoacclimation strategies in nature and their influence on P^b_{max}.

Nutrient Limitation

The PhotoAcc model employs a simple switch between nutrient 'charged' and 'depleted' models, rather than a more gradual transition as a function of nutrient stress. Falkowski et al. (1989) reported a similar switch in the ratio of photosynthetic electron transport (PET) components and Rubisco for *Isochrysis galbana* grown under 9 different levels of nitrogen limitation in chemostats. Increasing nutrient stress (i.e., decreasing growth rates) decreased cellular concentrations of all measured components, with a constant stoichiometry for growth rates between 0.59 d^{-1} and 0.96. At growth rates < 0.59 d^{-1}, the relationship between PET components and Rubisco abruptly changed by 60% to a new equilibrium (Fig. 7). The magnitude of this shift is similar to the decrease in P^b_{max} predicted by the nutrient 'depleted' PhotoAcc model for moderate to high light. We are unaware of any physiological explanation for such abrupt changes and few laboratory studies have specifically addressed this problem.

Nutrient conditions represented by the AMT and BATS studies were nutrient 'charged',

phosphate 'depleted' (BATS) (Michaels et al. 1994; Michaels et al. 1996), and possibly nitrogen 'depleted' (AMT-2). We anticipate that additional modifications to equations 5 and 6 will be required to model P^b_{max} in iron limited regions. Iron limitation causes unique stoichiometeric changes in the composition of the photosystems, most notably a decrease in cytochrome b_6f and a higher photosystem II to photosystem I (PSII:PSI) ratio (Guikema and Sherman 1983; Sandmann 1985; Greene et al.1992; Straus 1994; Vassiliev et al. 1995; Behrenfeld and Kolber 1999). A high PSII:PSI ratio will diminish chlorophyll-specific efficiencies for conversion of photochemical energy to reducing equivalents necessary for carbon fixation, thereby decreasing P^b_{max} relative to similar levels of growth limitation by nitrogen or phosphate.

Global Implementation

The immediate goal of the research described here was to develop an effective field-based *model* for P^b_{max}, whereas our broader objective is to establish a robust P^b_{opt} *algorithm* for estimating global oceanic primary production from satellite ocean color data. Implementing the PhotoAcc model will require temporally resolved mixed layer depth and nutrient depletion fields. As an initial attempt, monthly climatological fields can be assembled from historical data sets (e.g., National Oceanographic Data Center), but eventually data coincident with satellite ocean color measurements will be preferred. Data assimilation models may be one potential approach for generating coincident mixed layer fields. Alternatively, research is now underway to investigate remote sensing lidar techniques for real-time measurements of mixed layer depths. Combining remotely sensed sea surface temperature fields with nutrient-depletion-temperature relationships may prove useful for assessing temporal changes in nutrient status. Again, data

assimilation models may provide an alternative technique. A variety of approaches may therefore be explored for implementing the PhotoAcc model and present an exciting challenge for future research.

Perspective

Deciphering decadal-scale changes in oceanic primary production from the much larger amplitude signals of seasonal and interannual variability requires foremost a long-term commitment to remote sensing programs monitoring changes in plant biomass, as well as process oriented models of depth-dependent changes in phytoplankton biomass and assimilation efficiencies. . An evolution from empirical to analytical models of phytoplankton photosynthesis has been realized primarily in the spectral description of the underwater light field (e.g., Platt and Sathyendranath 1988; Morel 1991; Platt et al. 1991; Antoine et al. 1996). Demonstrable improvements in model performance from these achievements have, unfortunately, been masked by the overwhelming influence of ineffective local scale models of physiological variability (Balch et al. 1992; Behrenfeld and Falkowski 1997a,b; Siegel et al. 2000). The PhotoAcc model presented here provides a framework for future improvements in the analytical characterization of physiological variability and, based on comparisons with AMT and BATS data, already incorporates two critical forcing factors: light and nutrients.

The importance of environmental physical-chemical variability on physiological traits of algae is well illustrated in the BATS data by the correspondence between changes in P^b_{opt} and the temporal rhythm of seasonal mixing and stratification (Fig. 5). Nutrient availability at this site generally influenced light-saturated photosynthesis at the seasonal scale, whereas higher

frequency variations in P^b_{opt} were dominated by photoacclimation responses to changes in mixed layer depth, surface PAR, and phytoplankton biomass (due to associated changes in vertical light attenuation). The BATS data also suggest a significance in the recent history of a water column, as the occasional mid-summer switches between nutrient 'depleted' and nutrient 'charged' P^b_{opt} values conceivably reflected the passing of a mesoscale eddy with a significantly different history than the water masses sampled the month before and after.

The conceptual basis of the PhotoAcc model presents a variety of hypotheses regarding sources of variability in light-saturated, chlorophyll-normalized photosynthetic rates. These include a dominant kinetic response to low-light exposure over high-light, an irradiance-dependence of the Calvin cycle capacity under chronic low light and nutrient limiting conditions, a nutrient-dependent switch in the stoichiometric relationship between light-harvesting and Calvin cycle components, and the temperature-independence of P^b_{max} above 5°C in natural phytoplankton assemblages. Additional field and laboratory studies will be necessary to test these hypotheses and to expand the PhotoAcc model to encompass iron limiting conditions, temperature effects at < 5°C, and possibly species-dependent variability in phytoplankton pigment composition.

ACKNOWLEDGMENTS

M.J. Behrenfeld thanks Ricardo Letelier, Paul Falkowski, Richard Geider, and Zbigniew Kolber for helpful discussions and inspiration, Elizabeth Stanley for encouragement, and the U.S. National Aeronautics and Space Administration (NASA) (grant #UPN161-35-05-08) for it's continued support. BATS data were assembled by Toby Westberry and Margaret O'Brien. The U.S. JGOFS BATS program is supported by the National Science Foundation. D.A. Siegel's contributions were supported by NASA. E. Marañón thanks Manuel Varela and Beatriz Mouriño for assistance during the AMT studies and Alan Pomroy, Colin Griffiths and Malcolm Woodward for providing nutrient data. S.B. Hooker thanks J. Brown, C. Dempsey, S. Maritorena, and G. Moore for AMT support and J. Aiken for his diligence and commitment to supporting high quality AMT optical data.

REFERENCES

Antoine, D., J-M. André and A. Morel. 1996. Oceanic primary production 2. Estimation at global scale from satellite (coastal zone color scanner) chlorophyll. Global Biogeochem. Cycles **10:** 57-69.

Balch, W., R. Evans, J. Brown, G. Feldman, C. McClain and W. Esaias. 1992. The remote sensing of ocean primary productivity: Use of new data compilation to test satellite models. J. Geophys. Res. **97(C2):** 2279-2293.

Balch, W. M. and C. F. Byrne. 1994. Factors affecting the estimate of primary production from space. J. Geophys. Res. **99(C4):** 7555-7570.

Banse, K. and M. Yong. 1990. Sources of variability in satellite-derived estimates of phytoplankton production in the Eastern Tropical Pacific. J. Geophys. Res. **95(C5):** 7201-7215.

Beale, S.I. and D. Appleman. 1971. Chlorophyll synthesis in *Chlorella*: Regulation by degree of light limitation of growth. Plant Physiol. **47:** 230-235.

Beardall, J and I. Morris. 1976. The concept of light intensity adaptation in marine phytoplankton: some experiments with *Phaeodactylum tricornutum*. Mar. Biol. **37:** 377-387.

Behrenfeld, M.J. and P.G. Falkowski. 1997a. A consumer's guide to phytoplankton primary

productivity models. Limnol. Oceanogr. **42:** 1479-1491.

Behrenfeld, M.J. and P.G. Falkowski. 1997b. Photosynthetic rates derived from satellite-based chlorophyll concentration. Limnol. Oceanogr. **42:** 1-20

Behrenfeld, M.J., O. Prasil, Z.S. Kolber, M. Babin and P.G. Falkowski. 1998. Compensatory changes in photosystem II electron turnover rates protect photosynthesis from photoinhibition. Photosynth. Res. **58:** 259-268

Behrenfeld, M.J. and Z.S. Kolber. 1999. Widespread iron limitation of phytoplankton in the south Pacific ocean. Science **283:** 840-843.

Chan, A.T. 1978. Comparative physiological study of marine diatoms and dinoflagellates in relation to irradiance and cell size. I. Growth under continuous light. J. Phycol. **14:** 396-402.

Cosper, E. 1982a. Effects of variations in light intensity on the efficiency of growth of *Skeletonema costatum* (Bacillariophyceae) in a cyclostat. J. Phycol. **18:** 360-368.

Cosper, E. 1982b. Influence of light intensity on diel variation in rates of growth, respiration, and organic release of a marine diatom: comparison of diurnally constant and fluctuating light. J. Plankt. Res. **4:** 705-724.

Cullen, J.J. and M.R. Lewis. 1988. The kinetics of algal photoacclimation in the context of vertical mixing. J. Plankt. Res. **10:** 1039-1063.

Dierssen, H.M., M. Vernet and R.C. Smith. 2000. Optimizing models for remotely estimating primary production in Antarctic coastal waters. Antarct. Sci. In press.

Dubinsky, Z., P.G. Falkowski and K. Wyman. 1986. Light harvesting and utilization by phytoplankton. Plant Cell Physiol. **27:** 1335-1349.

Durbin, E.G. 1974. Studies on the autecology of the marine diatom *Thalassiosira nordenskiöldii* cleve: I. The influence of daylength, light intensity, and temperature on growth. J. Phycol. **10:** 220-225.

Eppley, R. W. 1972. Temperature and phytoplankton growth in the sea. Fish. Bull. **70:** 1063-1085.

Eppley, R.W. and P.R. Sloan. 1966. Growth rate of marine phytoplankton: Correlations with light absorption by cell chlorophyll. Physiol. Plant. **19:** 47-59.

Escoubas, J-M., M. Lomas, J. LaRoche and P.G. Falkowski. 1995. Light intensity regulation of cab gene transcription is signaled by the redox state of the plastoquinone pool. Proc. Natl. Acad. Sci. **92:** 10237-10241.

Falkowski, P.G. 1980. Light-shade adaptation in marine phytoplankton. *In:* Falkowski, P.G. [ed]. Primary production in the Sea. Plenum pp. 99-119.

Falkowski, P.G. and T.G. Owens. 1980. Light-shade adaptation. Plant Physiol. **66:** 592-595.

Falkowski, P. G. 1981. Light-shade adaptation and assimilation numbers. J. Plankton Res. **3:** 203-216.

Falkowski, P.G., T.G. Owens, A.C. Ley and D.C. Mauzerall. 1981. Effects of growth irradiance levels on the ratio of reaction centers in two species of marine phytoplankton. Plant Physiol. **68:** 969-973.

Falkowski, P.G. and C.D. Wirick. 1981. A simulation model of the effects of vertical mixing on primary production. Mar. Biol. **65:** 69-75.

Falkowski, P.G., A. Sukenik and R. Herzig. 1989. Nitrogen limitation in *Isochrysis galbana* (Haptophyceae). II. Relative abundance of chloroplast proteins. J. Phycol. **25:** 471-478.

Faust, M.A., J.C. Sager and B.W. Meeson. 1982. Response of *Prorocentrum mariae-lebouriae* (Dinophyceae) to light of different spectral qualities and irradiances: Growth and pigmentation. **18:** 349-356.

Field, C.B., M.J. Behrenfeld, J.T. Randerson and P.G. Falkowski. 1998. Primary production of the biosphere: Integrating terrestrial and oceanic components. Science **281:** 237-240

Geider, R.J., B.A. Osborne and J.A. Raven. 1985. Light dependence of growth and photosynthesis in *Phaeodactylum tricornutum* (Bacillariophyceae). J. Phycol. **21:** 609-619.

Geider, R.J., B.A. Osborne and J.A. Raven. 1986. Growth, photosynthesis and maintenance metabolic cost in the diatom *Phaeodactylum tricornutum* at very low light levels. J. Phycol. 22: 39-48.

Geider, R.J. 1987. Light and temperature dependence of the carbon to chlorophyll ratio in micgroalgae and cyanobacteria: Implications for physiology and growth of phytoplankton. New. Phytol. **106:** 1-34.

Geider, R.J., H.L. MacIntyre and T.M. Kana. 1996. A dynamic model of photoadaptation in phytoplankton. Limnol. Oceanogr. **41:**1-15.

Glover, H.E. 1980. Assimilation numbers in cultures of marine phytoplankton. J. Plankt. Res. **2:** 69-79.

Goericke, R. and N. A. Welschmeyer. 1992. Pigment turnover in the marine diatom *Thalassiosira weisflogii.* I. The $^{14}CO_2$-labeling kinetics of chlorophyll. J. Phycol. **28:** 498-507.

Greene, R.M., R.J. Geider, Z. Kolber and P.G. Falkowski. 1992. Iron-induced changes in light harvesting and photochemical energy conversion processes in eukaryotic marine algae. Plant Physiol. **100:** 565-575..

Guikema, J.A. and L.A. Sherman 1983. Organization and function of chlorophyll in membranes of cyanobacteria during iron starvation. Plant Phys. **73:** 250–256.

Harris, G.P. 1978. Photosynthesis, productivity, and growth: The physiological ecology of phytoplankton. *In:* Elster, H.-J. And Ohle, W. [eds.] Ergebnisse der limnologie. Archiv für Hydrobiologie. Stuttgart.

Heber, U., Neimanis, S. and K.-J. Dietz. 1988. Fractional control of photosynthesis by the Q_B protein, the cytochrome f/b_6 complex and other components of the photosynthetic apparatus. Planta **173:** 267-274.

Hood, R. R., M. R. Abbott and A. Huyer. 1991. Phytoplankton and photosynthetic light response in the coastal transition zone of northern California in June 1987. J. Geophys. Res. **96:** 14,769-14,780

Hooker, S.B. and S. Maritorena, 2000. An Evaluation of Oceanographic Optical Instruments and Deployment Methodologies. J. Atmos. and Oceanic Tech. (in press).

Knap, A.H. et al. 1993. BATS Methods - March 1993, BATS Method Manual Version 3. Woods Hole MA: U.S. JGOFS Planning and Coordination Office.

Kok, B. 1956. On the inhibition of photosynthesis by intense light. Biochim. Biophys. Acta **21:** 234-244.

Lapointe, B.E., C.J. Dawes and K.R. Tenore. 1984. Interaction between light and temperature on the physiological ecology of *Gracilaria tikvahiae*. Mar. Biol. **80:** 171-178.

Leverenz, J.W., S. Falk, C-M. Pilström and G. Samuelsson. 1990. The effects of photoinhibition on the photosynthetic light-response curve of green plant cells (*Chlamydomonas reinhardtii*). Planta **182:** 161-168.

Lewis, M.R., J.J. Cullen and T. Platt. 1984. Relationship between vertical mixing and photoadaptation of phytoplankton: similarity criteria. Mar. Ecol. Prog. Ser. **15:** 141-149.

Longhurst, A., S. Sathyendranath, T. Platt and C. Caverhill. 1995. An estimate of global primary production in the ocean from satellite radiometer data. J. Plankton Res. **17(6):** 1245-1271.

Longhurst, A. 1995. Seasonal cycles of pelagic production and consumption. Prog. Oceanogr. **36:** 77-167.

Malone, T.C., C. Garside and P.J. Neale. 1980. Effects of silicate depletion on photosynthesis by diatoms in the plume of the Hudson river. Mar. Biol. **58:** 197-204.

Marañón, E. and P.M. Holligan. 1999. Photosynthetic parameters of phytoplankton from 50°N to 50°S in the Atlantic ocean. Mar. Ecol. Prog. Ser. **176:** 191-203.

Marañón, E., P.M. Holligan, M. Varela, B. Mouriño and A. Bale. 2000. Basin-scale variability of phytoplankton biomass, production, and growth in the Atlantic ocean. Deep-Sea Res. Part I. **47:** 825-857.

Megard, R.O. 1972. Phytoplankton, photosynthesis, and phosphorus in Lake Minnetonka, Minnesota. Limnol. Oceanogr. **17:** 68-87.

Michaels, A.F., A.H. Knap, R.L. Dow, K. Gundersen, R.J. Johnson, J. Sorensen, A. Close, G.A. Knauer, S.E. Lohrenz, W.A. Asper, M. Tuel and R. Bidigare. 1994. Seasonal patterns of ocean biogeochemistry at the United States JGOFS Bermuda Atlantic time-series study site. Deep-Sea Res. Part I. **41:** 1013-1038.

Michaels, A.F. and A.H. Knap. 1996. Overview of the U.S. JGOFS Bermuda Atlantic Time-series Study and the Hydrostation S program. Deep-Sea Res. Part II. **43:** 157-198

Michaels, A.F., D. Olson, J.L. Sarmiento, J.W. Ammerman, K. Fanning, R. Jahnke, A.H. Knap,

F. Lipschultz and J.M. Prospero. 1996. Inputs, losses, and transformations of nitrogen and phosphorous in the pelagic north Atlantic ocean. Biogeochem. **35:** 181-226.

Morel, A. and J.-F. Berthon. 1989. Surface pigments, algal biomass profiles, and potential production of the euphotic layer: Relationships reinvestigated in view of remote-sensing applications. Limnol. Oceanogr. **34:** 1,545-1,562.

Morel, A. 1991. Light and marine photosynthesis: A spectral model with geochemical and climatological implications. Prog. Oceanogr. **26:** 263-306.

Morris, I. 1981. Photosynthetic products, physiological state, and phytoplankton growth. *In:* Platt, T. [ed]. Physiological basis of phytoplankton ecology.

Myers, J. 1946. Culture conditions and the development of the photosynthetic mechanism. J. Gen. Phsiol. **29:** 419-427.

Orellana, M.V. and M.J. Perry. 1992. An immunoprobe to measure Rubisco concentrations and maximal photosynthetic rates of individual phytoplankton cells. Limnol. Oceangr. **37:** 478-490.

Paasche, E. 1967. Marine plankton algae grown with light-dark cycles. I. *Coccolithus huxleyi.* Physiol. Plant. **20:** 946-956.

Paasche, E. 1968. Marine plankton algae grown with light-dark cycles. II. *Ditylum brightwellii* and *Nitzschia turgidula*. Physiol. Plant. **21:** 66-77.

Platt, T. and S. Sathyendranath. 1988. Oceanic primary production: Estimation by remote sensing at local and regional scales. Science **241:** 1613-1620.

Platt, T., C. Caverhill and S. Sathyendranath. 1991. Basin-scale estimates of oceanic primary production by remote sensing: The north Atlantic. J. Geophys. Res. **96:** 15,147-15,159.

Platt, T. and S. Sathyendranath. 1993. Estimators of primary production for interpretation of remotely sensed data on ocean color. J. Geophys. Res. **98:** 14,561-14,567.

Post, A.F., R. deWit and L.R. Mur. 1985. Interaction between temperature and light intensity on growth and photosynthesis of the cyanobacterium *Oscillatoria agardhii*. J. Plankt. Res. **7:** 487-495.

Raps, S., K. Wyman, H.W. Siegelman and P.G. Falkowski. 1983. Adaptation of the cyanobacterium *Microcystis aeruginosa* to light intensity. Plant Physiol. **72:** 829-832.

Richardson, K., J. Beardall and J.A. Raven. 1983. Adaptation of unicellular algae to irradiance: An analysis of strategies. New Phytol. **93:** 157-191.

Riper, D.M., T.G. Owens and P.G. Falkowski. 1979. Chlorophyll turnover in *Skeletonema costatum*, a marine plankton diatom. Plant Physiol. **64:** 49-54.

Robins, D.B., A.J. Bale, G.F. Moore, N.W. Rees, S.B. Hooker, C.P. Gallienne, A.G. Westbrook, E. Marañón, W.H. Spooner and S.R. Laney, 1996. AMT-1 Cruise Report and Preliminary Results. NASA Tech. Memo. 104566, Vol. 35, S.B. Hooker and E.R. Firestone [Eds.] NASA Goddard Space Flight Center, Greenbelt, Maryland, 87 pp.

Ryther, J.H. 1956. Photosynthesis in the ocean as a function of light intensity. Limnol. Oceanogr. **1:** 61-70.

Ryther, J.H. and C.S. Yentsch. 1957. The estimation of phytoplankton production in the ocean from chlorophyll and light data. Limnol. Oceanogr. **2:** 281-286.

Sandmann, G. 1985. Consequences of iron deficiency on photosynthetic and respiratory electron transport in blue-green algae. Photosynth. Res. **6:** 261-271.

Siegel, D.A., A.F. Michaels, J. Sorensen, M.C. O'Brien and M.A. Hammer. 1995a. Seasonal variability of light availability and its utilization in the Sargasso Sea. Journal of Geophysical Research, **100:** 8695-8713.

Siegel, D.A., M.C. O'Brien, J.C. Sorensen, D. Konnoff and E. Fields. 1995b. BBOP Data

Processing and Sampling Procedures. U.S. JGOFS Planning Report Number 19, U.S. JGOFS Planning and Coordination Office, 77 pp.

Siegel, D.A., T.K. Westberry, M.C. O'Brien, N.B. Nelson, A.F. Michaels, J.R. Morrison, A. Scott, E.A. Caporelli, J.C. Sorensen, S. Maritorena, S.A. Garver, E.A. Brody, J Ubante and M.A. Hammer. 2000. Bio-optical modeling of primary production on regional scales: The Bermuda biooptics project. Deep-Sea Res. Part II. In press.

Steemann Nielsen, E. 1952. The use of radio-active carbon (C^{14}) for measuring organic production in the sea. J. Cons. Cons. Int. Explor. Mer **18:** 117-140.

Steemann Nielsen, E. and V. Kr. Hansen. 1959. Light adaptation in marine phytoplankton populations and its interrelation with temperature. Physiol. Plant. **12:** 353-370.

Steemann Nielsen, E. and E.G. Jørgensen. 1968. The adaptation of plankton algae: I. General part. Physiol. Plant. **21:** 401-413.

Stitt, M. 1986. Limitation of photosynthesis by carbon metabolism, I. Evidence for excess electron transport capacity in leaves carrying out photosynthesis in saturating light and CO_2. Plant Physiol. **81:** 1115-1122.

Straus, N.A. 1994. Iron Deprivation: Physiology and gene regulation. *In:* D.A. Bryant [ed.] The

Molecular Biology of Cyanobacteria. (Kluwer Academic, 1994) pp. 731-750

Sukenik, A., J. Bennett and P.G. Falkowski. 1987. Light-saturated photosynthesis-limitation by electron transport or carbon fixation? Biochim. Biophys. Acta **891:** 205-215.

Talling, J.F. 1957. The phytoplankton population as a compound photosynthetic system. New. Phytol. **56:**133-149.

Terry, K.L., J. Hirata and E.A. Laws. 1983. Light-limited growth of two strains of the marine diatom *Phaeodactylum tricornutum* Bohlin: Chemical composition, carbon partitioning, and the diel periodicity of physiological processes. J. Exp. Mar. Biol. Ecol. **68:** 209-227.

Vassiliev, I.R., Z. Kolber, K.D. Wyman, D. Mauzerall, V.K. Shukla and P.G. Falkowski. 1995. Effects of iron limitation on photosystem II composition and light utilization in *Dunaliella tertiolecta* Plant Physiol. **109:** 963-972

Verity, P.G. 1981. Effects of temperature, irradiance, and daylength on the marine diatom *Leptocylindrus danicus* cleve: I. Photosynthesis and cellular composition. J. Exp. Mar. Biol. Ecol. **55:** 79-91.

Vincent, W.F., N. Bertrand and J.-F. Frenette. 1994. Photoadaptation in intermittent light across the St. Lawrence estuary freshwater-saltwater transition zone. Mar. Ecol. Prog. Ser. **110:** 283-

292.

Weinbaum, S.A., J. Gressel, A. Reisfeld and M. Edelman. 1979. Characterization of the 32,000 Dalton chloroplast membrane protein: probing its biological function in *Spirodela*. Plant Physiol. **64:** 828-832.

Wright, J.C. 1959. Limnology of Canyon Ferry Reservoir: Phytoplankton standing crop and primary production. Limnol. Oceanogr. **4:** 235-245.

Yoder, J.A. 1979. Effect of temperature on light-limited growth and chemical composition of *Skeletonema costatum* (Bacillariophyceae). J. Phycol. **15:** 362-370.

FIGURE LEGENDS

Fig. 1 Compilation of published studies reporting a relationship between chlorophyll concentration and growth irradiance (I_g). Chlorophyll concentrations were normalized to a scalar, yielding unitless relative values. The inset shows the full scale of relative chlorophyll concentrations and I_g. The solid line indicates a fit to the data following equation 1. Parameters for this fit (a = 0.036, b = 0.2, c = 1.15) differ from equation 3 because the PhotoAcc model describes changes in chlorophyll concentration relative to the Calvin cycle capacity, rather than relative chlorophyll per cell. The PhotoAcc model is also based on units of mol quanta m^{-2} s^{-1}, rather than μmol quanta m^{-2} s^{-1}. These data were compiled to show the general trend between chlorophyll and I_g, but do not represent an exhaustive review of all published results. Data sources and species tested are as follows, with outliers excluded from figure 1 identified in brackets by incubation temperature (°C), photoperiod (h),and growth irradiance (μmol quanta m^{-2} s^{-1}): Myers (1946) *Chlorella pyrenoidosa*; Eppley and Sloan (1966) *Dunaliella tertiolecta* [16 h, 49 μmol quanta m^{-2} s^{-1}]; Paasche (1967), *Coccolithus huxleyi*; Paasche (1968), *Ditylum brightwellii* [10 h, 244 μmol quanta m^{-2} s^{-1}], *Nitzschia turgidula*; Beale and Appleman (1971) *Chlorella vulgaris*; Durbin (1974) *Thalassiosira nordenskioldii* [5°C, 15 h, 195 μmol quanta m^{-2} s^{-1}; 10°C, 15 h, 31 μmol quanta m^{-2} s^{-1}; 15°C, 9 h, 195 μmol quanta m^{-2} s^{-1}]; Beardall and Morris (1976) *Phaeodactylum tricornutum*; Chan (1978) *Chaetoceros sp., Skeletonema costatum, Cylindrotheca fusiformis, Thalassiosira floridana* [8 μmol quanta m^{-2} s^{-1}], *Gymnodinium simplex, Amphidinium carterae*; Yoder (1979) *Skeletonema costatum* [22°C, 69 μmol quanta m^{-2} s^{-1}]; Falkowski and Owens (1980) *Skeletonema costatum, Dunaliella tertiolecta*; Falkowski (1980) *Dunaliella tertiolecta, Skeletonema*

costatum; Falkowski et al. (1981) *Dunaliella tertiolecta*; Verity (1981) *Leptocylindrus danicus* [15°C, 63 μmol quanta m^{-2} s^{-1}]; Cosper (1982a) *Skeletonema costatum*; Cosper (1982b) *Skeletonema costatum*; Faust et al. (1982) *Prorocentrum mariae-lebouriae*; Raps et al. (1983) *Microcystis aeruginosa*; Terry et al (1983) *Phaeodactylum tricornutum*; Geider et al. (1985) *Phaeodactylum tricornutum*; Post et al. (1985) *Oscillatoria agardhii*; Dubinski et al. (1986) *Thalassiosira weisflogii, Isochrysis galbana, Prorocentrum micans*; Sukenik et al. (1987) *Dunaliella tertiolecta*; Fisher (unpublished) *Tetraedron minimum, Nannochloropsis sp.*

Fig. 2 Relationships between irradiance (I_g) and relative chlorophyll concentration (– •• –), Calvin cycle capacity (— —), and the chlorophyll-normalized light-saturated photosynthetic rate (P^b_{max}) (solid line) assumed in the PhotoAcc model for (a) nutrient 'charged' and (b) nutrient 'depleted' conditions. P^b_{max} = the Calvin cycle capacity divided by chlorophyll concentration. The inset in (a) illustrates the low-light divergence between modeled Calvin cycle capacities for cells within the mixed layer (< MLD) and below the mixed layer depth (> MLD). Calvin cycle capacities are normalized with respect to mixed layer values under nutrient 'charge' conditions. Note change in vertical scales between (a) and (b).

Fig. 3 Results for the Atlantic Meridional Transect (a,c,e) AMT-3 and (b,d,f) AMT-2. Solid black symbols in all figures denote nutrient 'charged' conditions and gray symbols denote nutrient 'depleted' conditions. (a,b) Physical mixed layer depths (Z_M: ◆,◆) and nutricline depths (Z_N: ▽). Z_N was taken as the depth at which NO_3^- was first detectable or

assigned a value of 0 m when NO_3^- was elevated throughout the water column. (c-f) Comparison of measured (□) and modeled (●,●) chlorophyll-normalized light-saturated photosynthetic rates (P^b_{max}: mgC $mgChl^{-1}$ h^{-1}). (c,d) Mixed layer samples collected at 7 m depth. (e,f) Mid-depth samples generally collected below the mixed layer. ● = P^b_{max} estimated using the nutrient 'charged' PhotoAcc model. ● = P^b_{max} estimated using the nutrient 'depleted' PhotoAcc model (Fig. 2b). Comparison of measured versus modeled P^b_{max} for the combined AMT-3 and AMT-2 data (c-f) yielded a correlation coefficient (r^2) of 0.75.

Fig. 4 Exemplary vertical profiles of photosynthetically active radiation (PAR) (——), chlorophyll concentration (◆), NO_3^- (○), PO_4^{3-} (□), and sigma-theta (σ_t: ●) used to identify photoacclimation mixing depths (Z_{ACCL}: →). (a) A 'depleted' water column where NO_3^- and PO_4^{3-} concentrations are exhausted well below the mixing depth indicated by σ_t. In this case, Z_{ACCL} was the inflection depth of σ_t. (b) A typical 'charged' water column where all profiles indicate a similar depth for Z_{ACCL}. (c) An example of the infrequent condition where σ_t was vertically uniform, but NO_3^- and chlorophyll profiles indicated shallower mixing. In this case, Z_{ACCL} was set to the depth indicated by the NO_3^- profile. These exemplary profiles were extracted from the BATS data set (31° 50' N; 64° 10' W) on (a) 17 May, 1994, (b) 14 October, 1992, and (c) 12 December, 1996.

Fig. 5 PhotoAcc results for the 6 year Bermuda Atlantic Time-Series (BATS) record. (a) Measured (□) and modeled (●,●) optimal chlorophyll-normalized carbon fixation (P^b_{opt}:

mgC mgChl^{-1} h^{-1}) (r^2 = 0.82). P^b_{opt} was equated to the P^b_{max} value calculated by the PhotoAcc model. Model values were taken as the (●) nutrient 'charged' or (●) nutrient 'depleted' result (Fig. 2) best corresponding to measured P^b_{opt}. (b) Relationship between the physical mixed layer depth (Z_M: ◆,◆) and the depth of the nutricline (Z_N: ▽). Z_N was taken as the depth at which NO_3^- was first detectable or assigned a value of 0 m when NO_3^- was detected throughout the water column. NO_3^- was chosen as an index of nutrient 'charged' or 'depleted' conditions rather than PO_4^{3-} because the later was often undetectable even when Z_M was very large. ◆ = sampling dates when the 'charged' PhotoAcc model yielded the best results. ◆ = sampling dates when the 'depleted' PhotoAcc model yielded the best results.

Fig. 6 Measured P^b_{max} and P^b_{opt} (n = 181) versus modeled values from the temperature dependent functions of (a) Megard (1972) (r^2 = 0.06), (b) Balch et al. (1992) (r^2 = 0.04), (c) Antoine et al. (1996) (r^2 = 0.07), and (d) Behrenfeld and Falkowski (1997b) (r^2 = 0.01) and results for the PhotoAcc model (e) when switching was objectively based on the relationship between mixed layer and nutricline depths (r^2 = 0.64) and (f) when the best fit to observations was chosen from the nutrient 'depleted' and 'charged' models. Observational data are from the Atlantic Meridional Transect studies (AMT-2, AMT-3) and Bermuda Atlantic Time-Series study (BATS).

Fig. 7 Changes in photosynthetic electron transport (PET) components and Rubisco for *Isochrysis galbana* maintained in nitrogen-limited chemostats at growth rates ranging from 0.18 d^{-1} to 0.96 d^{-1}. Data are from Table 2 in Falkowski et al. (1989). PET

components: (▽) reaction center II (RCII), (◇) cytochrome-f, and (△) reaction center I. (●) Ratio of RCII:Rubisco. Data are normalized to the average value for the 4 highest growth rates.

Figure 1

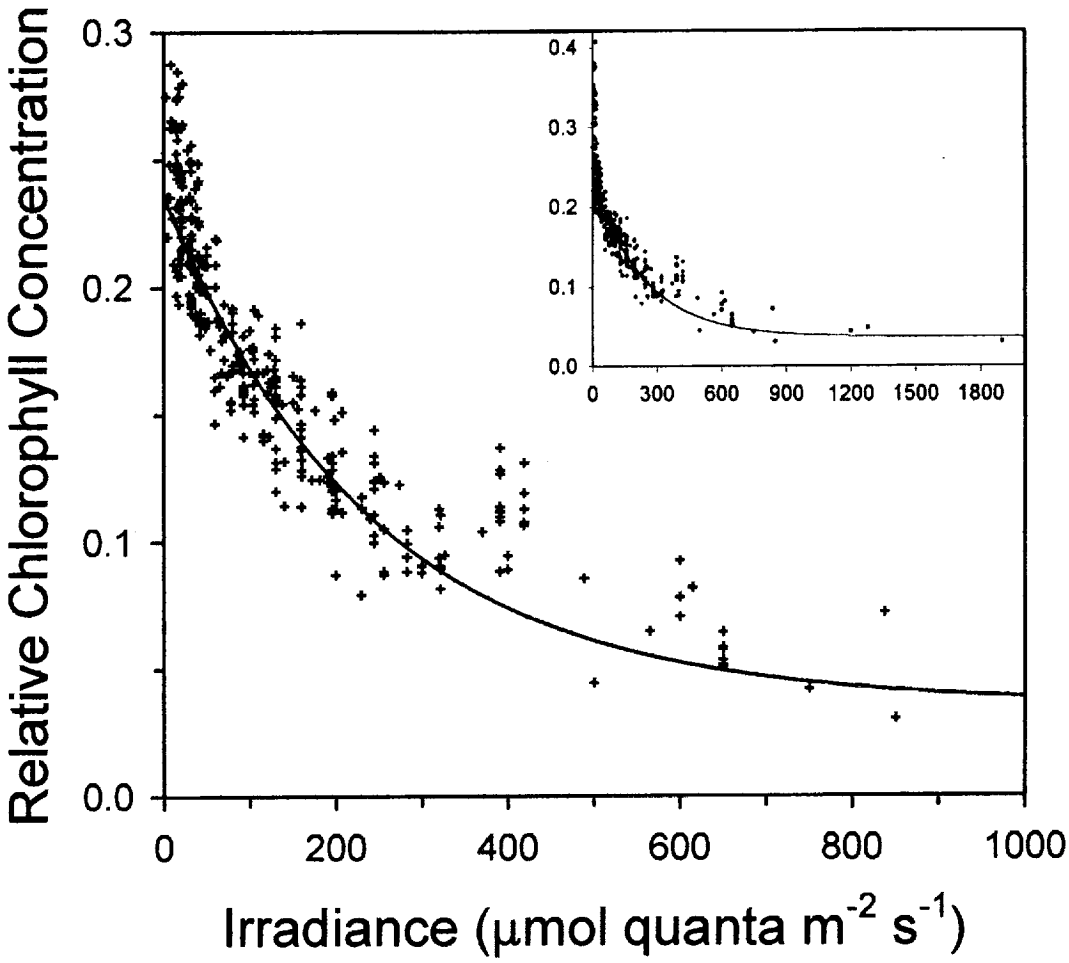
Relative Chlorophyll Concentration
0.3
0.2
0.1
0.0
0
200
400
600
800
1000
Irradiance (µmol quanta m-2 s-1)
0.4
0.3
0.2
0.1
0.0
0
300
600
900
1200
1500
1800

Figure 2

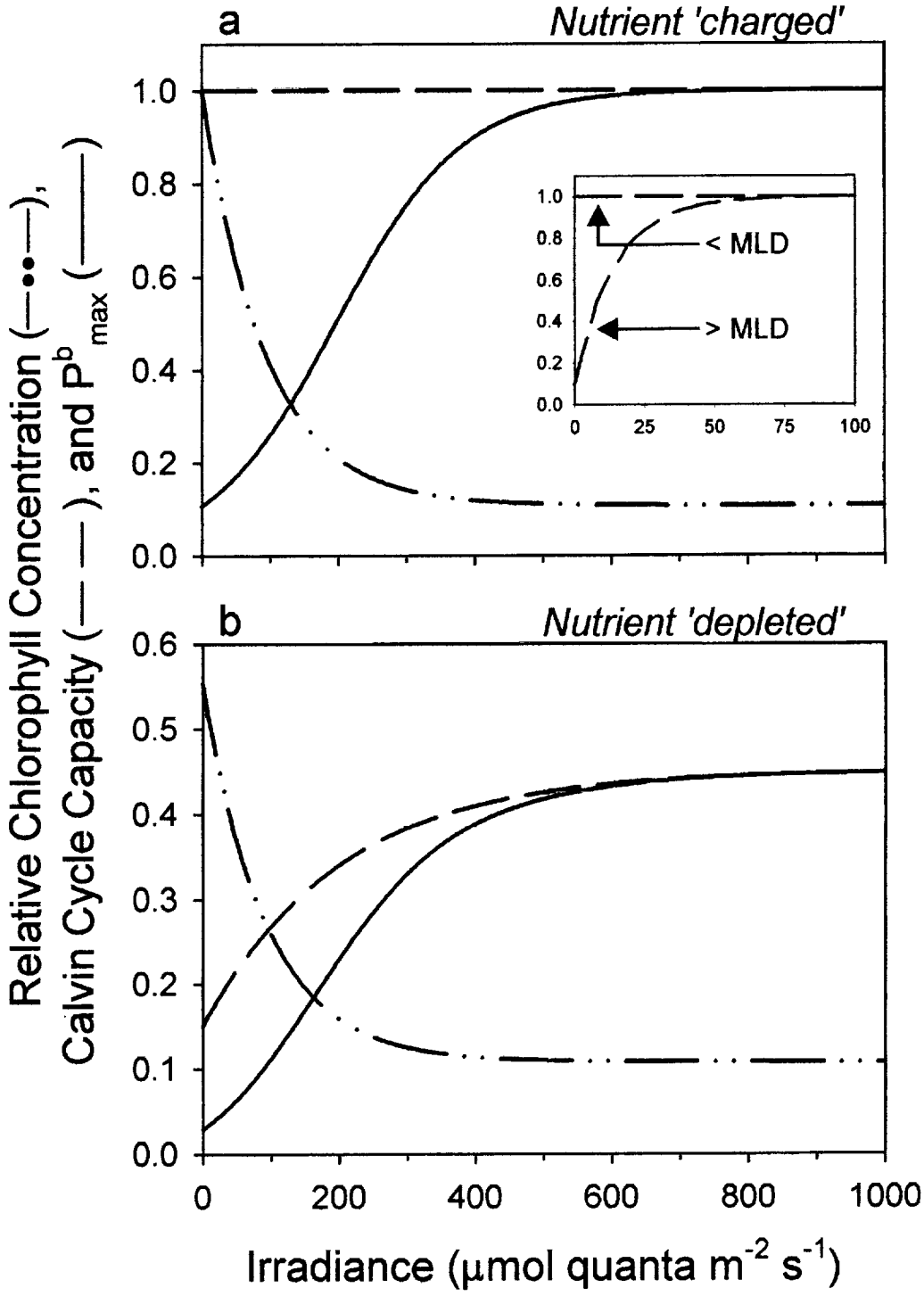
a
Nutrient 'charged'
b
Nutrient 'depleted'
< MLD
> MLD
Relative Chlorophyll Concentration (—•—),
Calvin Cycle Capacity (— — —), and P^b_{max} (———)
Irradiance (µmol quanta m^{-2} s^{-1})
0.0
0.2
0.4
0.6
0.8
1.0
0.1
0.3
0.5
0
200
400
600
800
1000
25
50
75
100

Figure 3

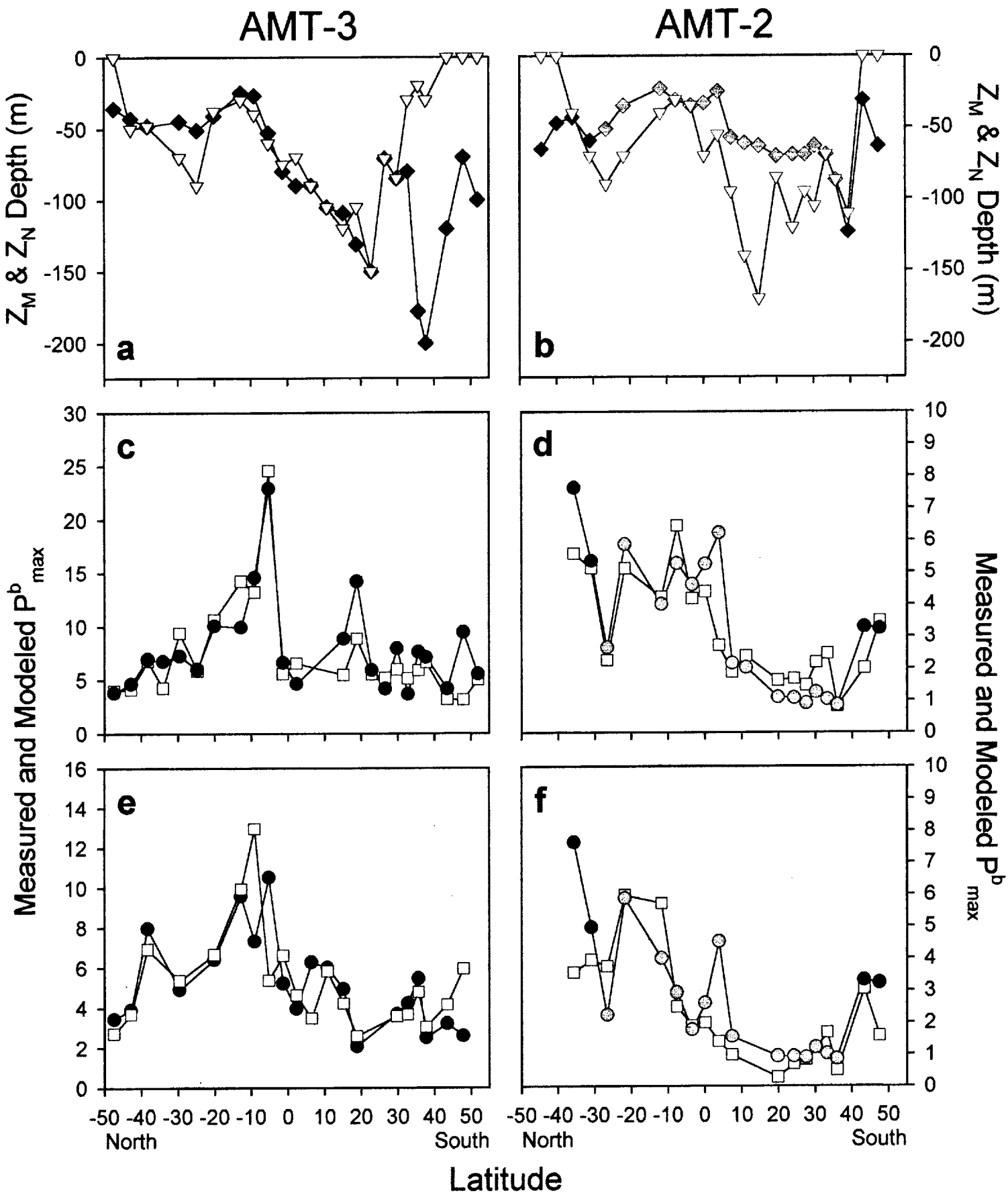
AMT-3
AMT-2
Z_M & Z_N Depth (m)
Z_M & Z_N Depth (m)
a
b
c
d
e
f
Measured and Modeled P^b_{max}
Measured and Modeled P^b_{max}
North
South
North
South
Latitude

Figure 4

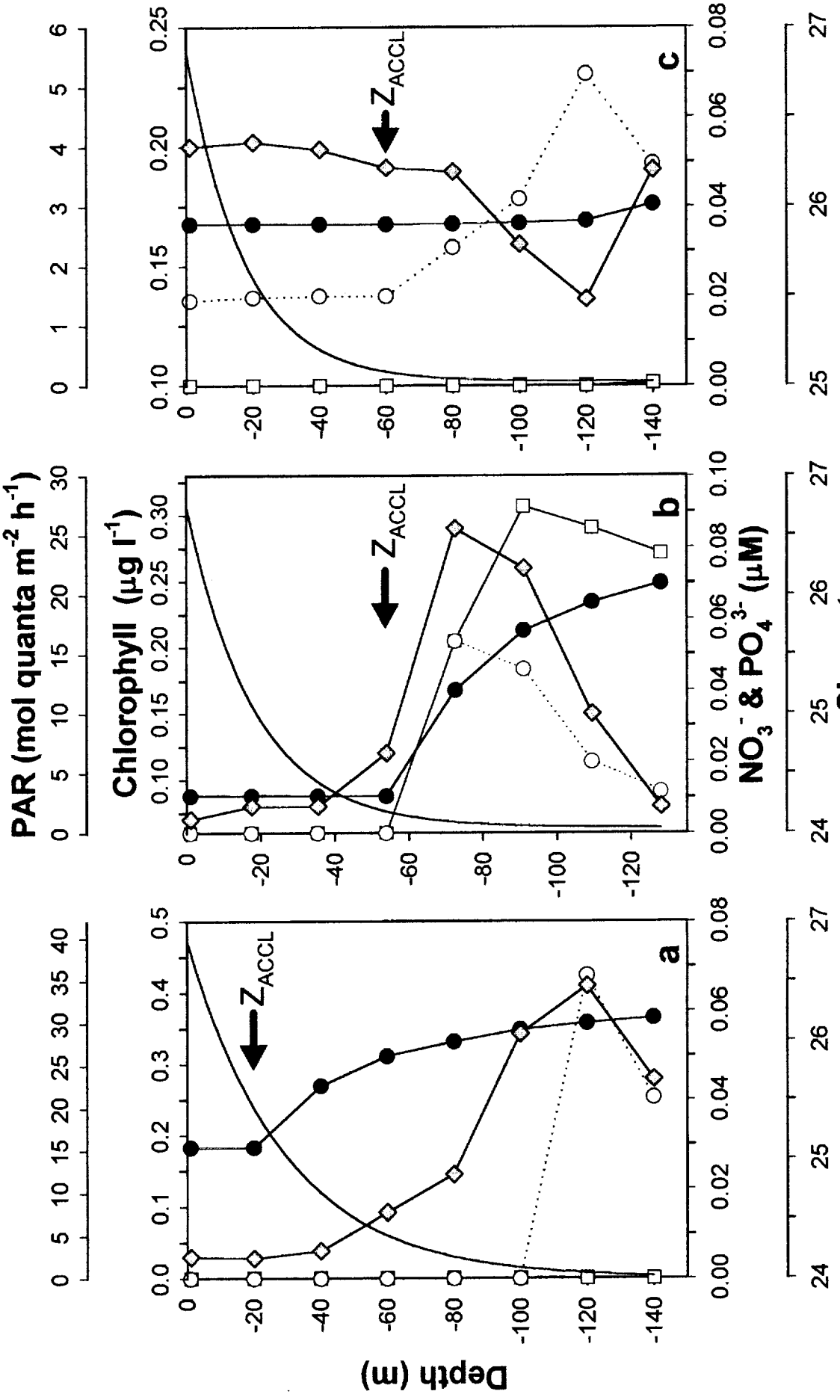
PAR (mol quanta m-2 h-1)
Chlorophyll (µg l-1)
NO3- & PO43- (µM)
Sigma-t
Depth (m)
ZACCL
a
b
c

Figure 5

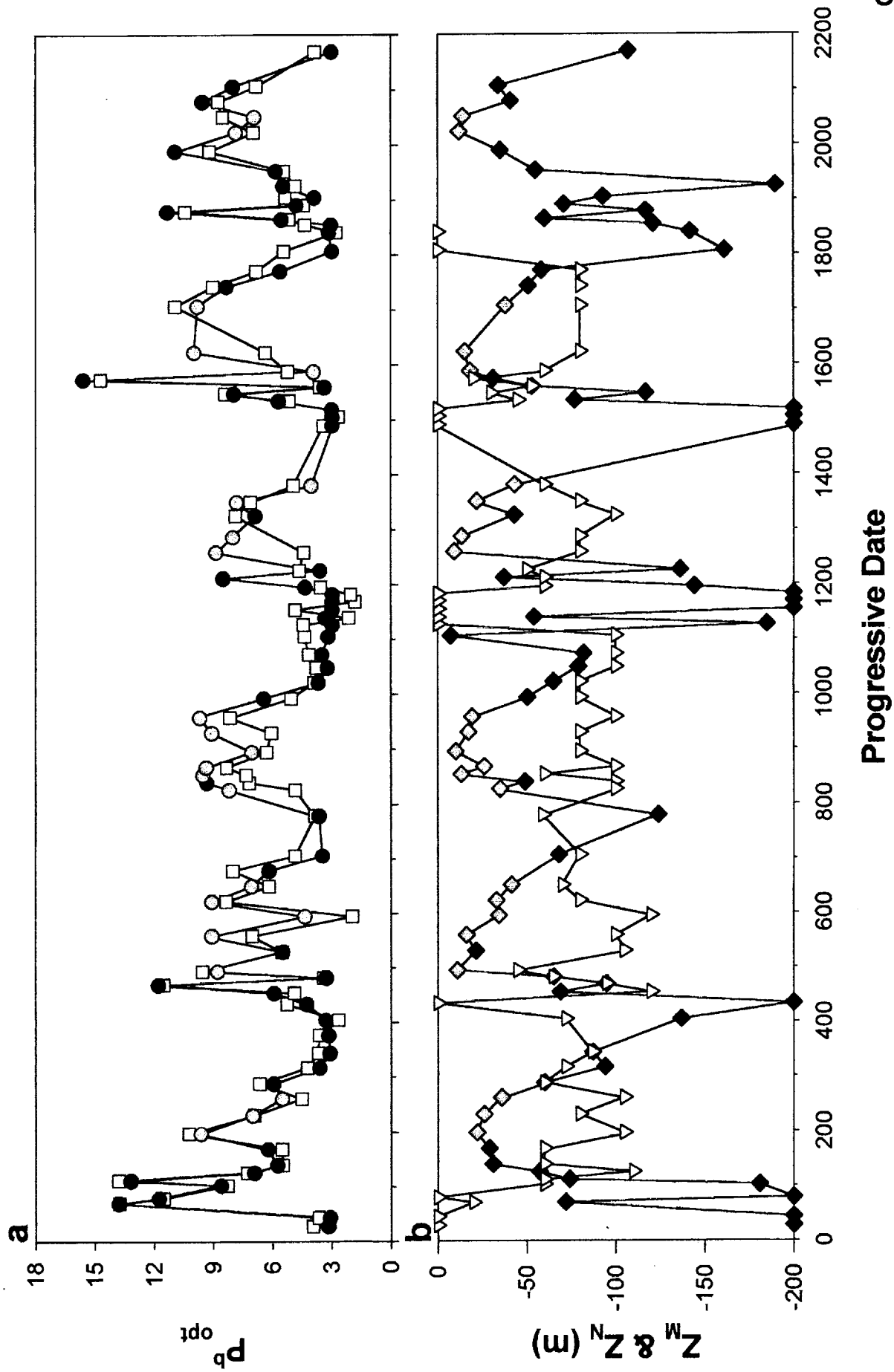
a
b
P^b_{opt}
Z_M & Z_N (m)
Progressive Date
18
15
12
9
6
3
0
0
-50
-100
-150
-200
0
200
400
600
800
1000
1200
1400
1600
1800
2000
2200

Figure 6

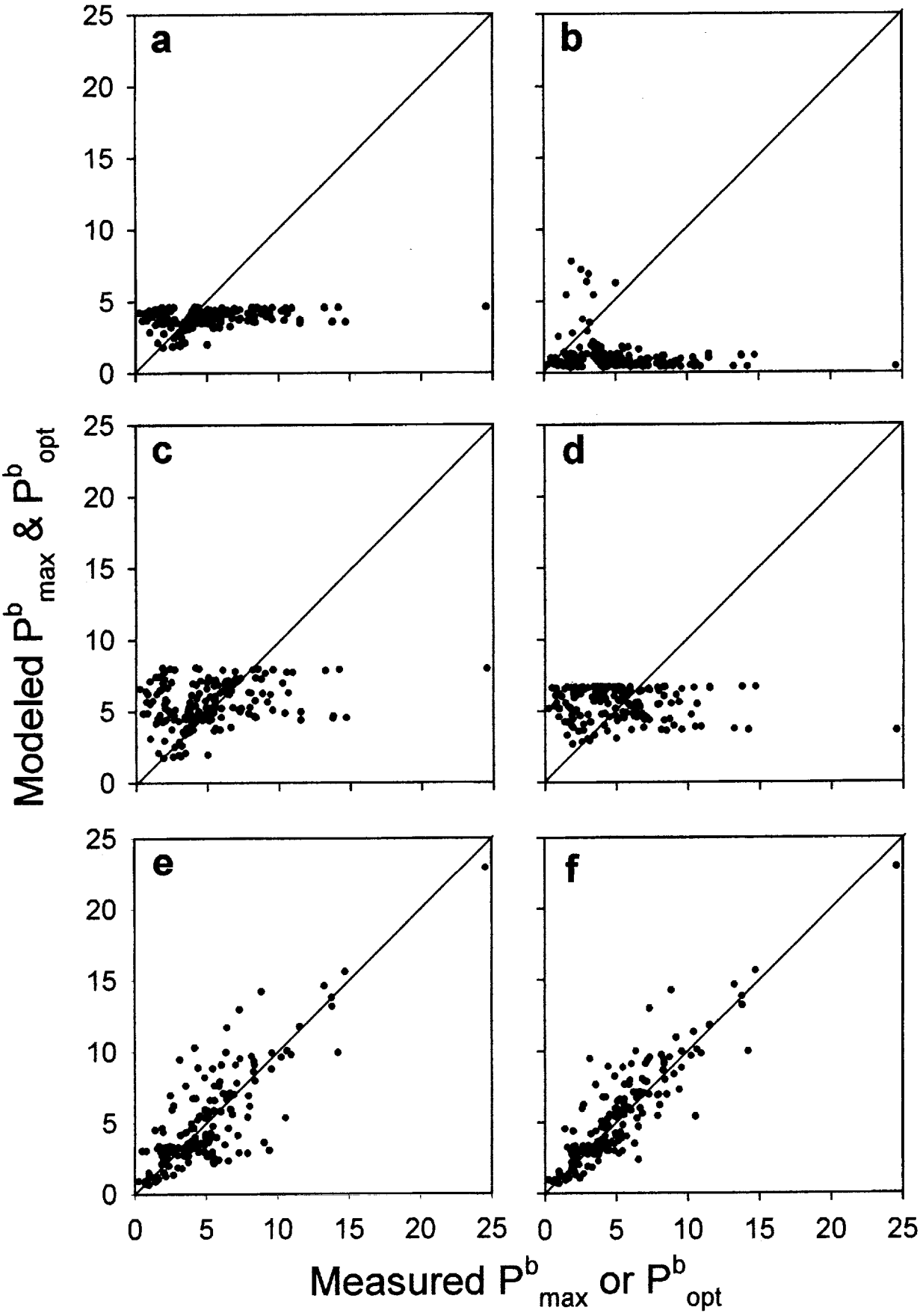
a
b
c
d
e
f
0
5
10
15
20
25
Modeled P^b_{max} & P^b_{opt}
Measured P^b_{max} or P^b_{opt}

Figure 7

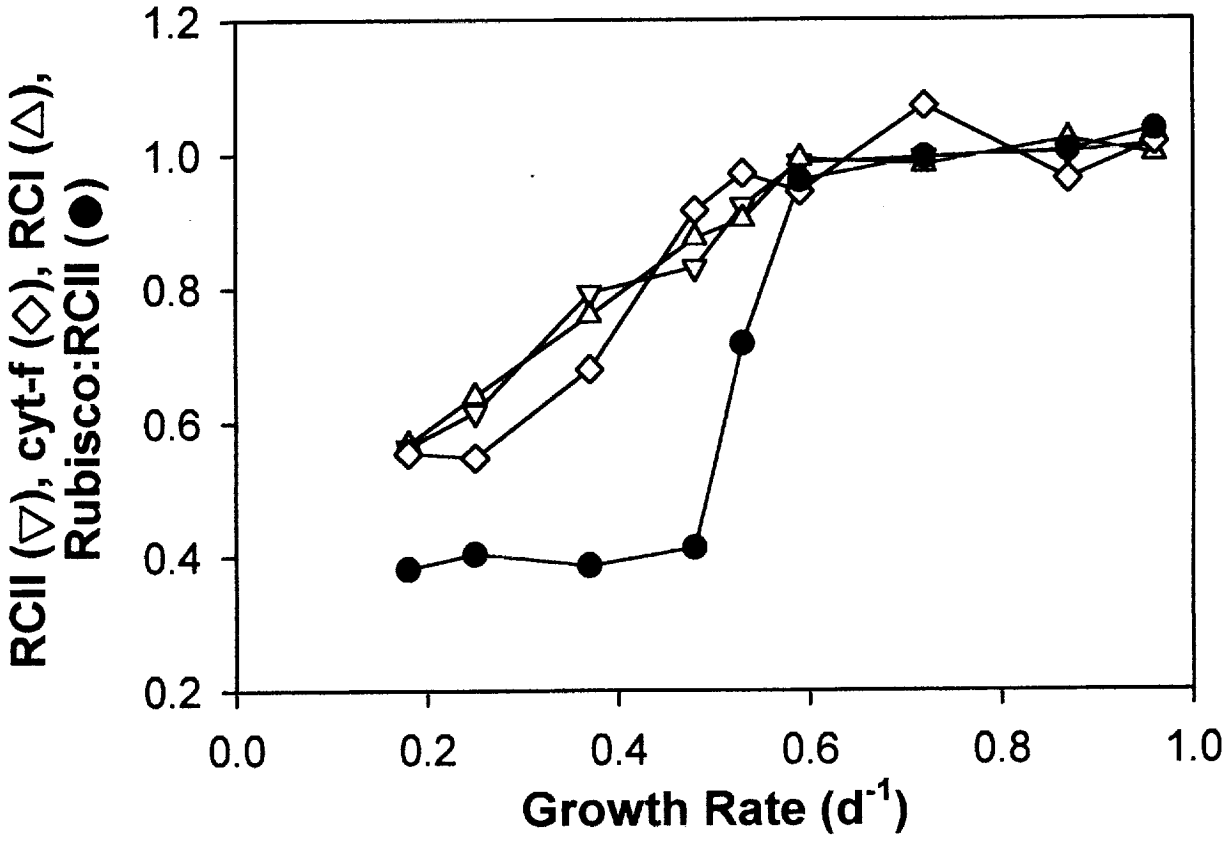
RCII (▽), cyt-f (◇), RCI (△), Rubisco:RCII (●)
1.2
1.0
0.8
0.6
0.4
0.2
0.0
0.2
0.4
0.6
0.8
1.0
Growth Rate (d-1)